Morphogenesis of Branched Coaxial Nanorods Formed in Supercritical Carbon Dioxide

Fangyu Cao,[†] Yeru Liu,[‡] Weihua Hu,[‡] and Qianwang Chen*[,‡,§]

Hefei National Laboratory for Physical Sciences at the Microscale and Department of Materials Science and Engineering, University of Science and Technology of China, Hefei 230026, Anhui, China

Received: July 15, 2007; In Final Form: November 15, 2007

Fe_3O_4/a-C branched and multibranched coaxial nanowires with a diameter around 40 nm were synthesized by pyrolysis of ferrocene in supercritical CO_2 at 450 °C. The single-crystal Fe_3O_4 cores of the coaxial nanowires are continuous. Every trunk, branch, and subbranch has a similar diameter, different from fractals, dendritics, or other hierarchical structures. The branches of the coaxial nanowires are vertical to the trunks, connected together with double-wedge junctions. The branched Fe_3O_4 core is a single crystal, with each branch having a growth orientation of ⟨100⟩, forming a three-dimensional framework-like three-divisional branched nanorod structure. A possible growth mechanism was proposed.

Introduction

Magnetic nanowires have attracted much attention because of their peculiar properties[1] and potential applications in functional nanodevices.[2] Nanowires of magnetic metals and their alloys have been prepared by electrochemical deposition.[3] However, they are easily oxidized in air and form an oxide layer, which limits their usefulness in practical applications. Magnetite is widely used in storage devices, gas sensors, biomedical treatment, and spintronic devices.[4] Now many ways have been developed for the synthesis of Fe_3O_4 nanowires, such as electroprecipitation in templates,[5] thermal decomposition,[6] and hydrothermal treatment.[7] The ways based on templates, such as porous anodic aluminum oxide, usually give polycrystalline nanowires,[5] and the templates used in the preparation cannot be removed completely. The other synthetic ways can produce single-crystalline nanowires, yet with a short aspect ratio.[7] Recently, we have developed a simple approach to synthesize core−shell Fe_3O_4/a-C without a catalyst, surfactants, or templates.[8]

In just the past decade, more complex structural architectures, such as heterostructures,[9] core−shell clusters and nanowires,[10] dendrites,[11] and branched nanowires,[12] offer other approaches and potentials for increasing structural complexity and enabling greater mechanical, optical, and electrical properties and function. Moreover, it is possible now to prepare semiconductor and metal nanocrystals with nearly monodisperse size distributions, to modify the structures with distinct shell coatings, and to have some degree of control over the shape.[13] However, to the best of our knowledge, synthesis of complex structures of magnetite such as dendrites or branched nanowires has not been reported yet.

Supercritical carbon dioxide ($ScCO_2$) has emerged as an important solvent in industrial applications because it is inexpensive, nonflammable, nontoxic, and environmentally friendly.[14] Recently, many carbon-based materials such as cubic diamond, carbon nanotubes, and Fe_3O_4/a-C core−shell nanowires were synthesized in an $ScCO_2$ system.[8,15] Herein, we report the growth of branched Fe_3O_4/a-C core−shell nanowires and dendrites via a simple one-pot process.

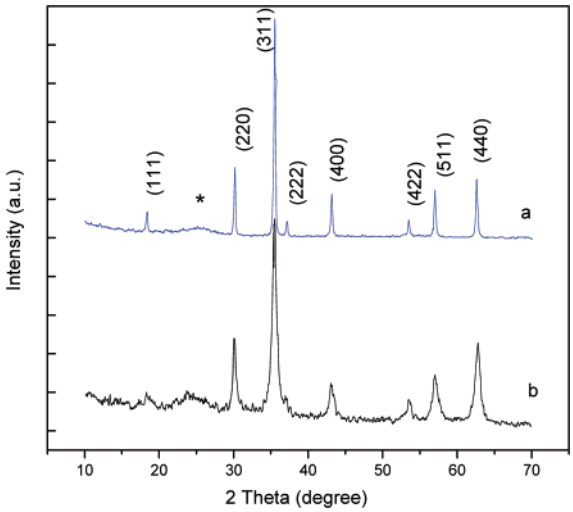

Figure 1. XRD of samples (a) CM450-1 and (b) CM450-6.

Experimental Section

All products were synthesized using a one-pot method. Ferrocene was used as an Fe and carbon source. A 0.25−1.00 g portion of the source material, together with 0.0−12.0 g of dry ice, was put into a 20 mL autoclave. The autoclave was then sealed quickly, heated to 450 °C, kept at that temperature for 600 min, and then naturally cooled to room temperature. After reaction, the inside wall of the autoclave was covered by dark brown-black powders.

The powder X-ray diffraction (XRD) analyses were performed on a Rigaku D/MAX-γA X-ray diffractometer equipped with Cu Kα radiation (λ = 1.541874 Å) over the 2θ range of 10−70°. Transmission electron microscopy (TEM) analyses were performed on a Hitachi H-800 transmission electron microscope with electron diffraction, and the accelerating potential was 200 kV. For TEM observations, the products were

* To whom correspondence should be addressed. E-mail: cqw@ustc.edu.cn.
[†] Department of Chemistry, University of Science and Technology of China.
[‡] Department of Materials Science and Engineering, University of Science and Technology of China.
[§] Hefei National Laboratory for Physical Sciences at the Microscale.

10.1021/jp0755342 CCC: $40.75
Published on Web 01/25/2008

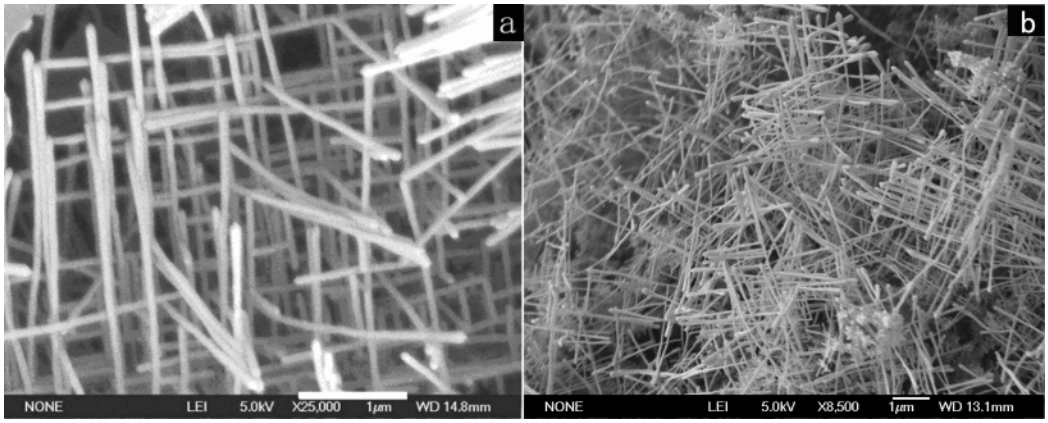

Figure 2. Typical FESEM images of sample CM450-1. The length of the bars is 1 μm.

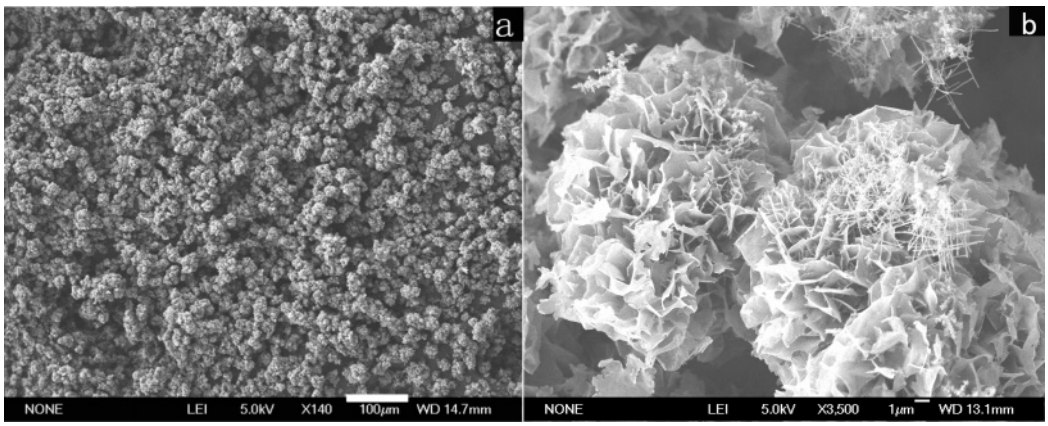

Figure 3. Typical FESEM image of sample CM450-6 (a) and magnified image of sample CM450-6 (b). The lengths of the bars in (a) and (b) are 100 and 1 μm, respectively.

TABLE 1: List of Samples

	factors in synthesis				
sample	ferrocene mass/g	CO_2 mass/g	T/°C	t/min	remarks
CM450-1	0.25	6.0	450	600	
CT450-1	0.25	6.0	450	600	product treated with HCl
CM450-2	0.25	3.0	450	600	
CM450-3	0.25	1.5	450	600	
CM450-4	0.25	0.0	450	600	
CM450-5	0.50	6.0	450	600	
CM450-6	1.00	6.0	450	600	
CM450-7	0.25	12.0	450	600	
CM450-W	0.25	6.0	450	600	0.5 g of H_2O added to the reaction system

separated in ethanol by ultrasonic dispersion and then transferred onto carbon-coated copper grids. Field emission scanning electron microanalysis (FESEM) was performed on a JEOL JSM-6700F field emission scanning electron microanalyzer. High-resolution transmission electron microscopy (HRTEM) images were taken on a JEOL-2010 with an accelerating voltage of 200 kV. Magnetic measurements were carried out on a Quantum Design superconducting quantum interference device (SQUID) (0 T $\leq H \leq$ 5 T) at room temperature (300 K).

Results and Discussion

Samples used in this study are listed in Table 1. Via a lot of experiments and analysis, we found sample CM450-1 as the best sample of branched/multibranched Fe_3O_4/a-C core−shell nanowires. Figure 1a shows the XRD pattern of the sample, in which the diffraction peaks of Fe_3O_4 were found. Marked with an asterisk in the XRD pattern, the diffraction of the amorphous species is relatively weak and almost invisible.

FESEM images of the samples are shown in Figures 2 and 3. A typical structure of the Fe_3O_4 nanomaterials in these samples is a branched coaxial nanowire, shown in Figure 2. In this sample, Fe_3O_4 shows a framework-like three-dimensional branched nanorod structure. Parallel or vertical with each other, every branch has a similar diameter, making it hard to distinguish the branches from the trunks, branches, subbranches, and so on. This makes the structure different from the reported dendritic, polycrystalline fractal, or hierarchical structures.[11−13,16] From Figure 2b, we may find that this kind of branched nanorod is abundant in sample CM450-1, the main constituent of which is FC magnetite, integrated with the XRD pattern of the sample in Figure 1a. The corresponding TEM image (Figure 4a) shows that the nanorods are of a kind of coaxial structure, with the Fe_3O_4 nanorod as the core and amorphous carbon the shell. The

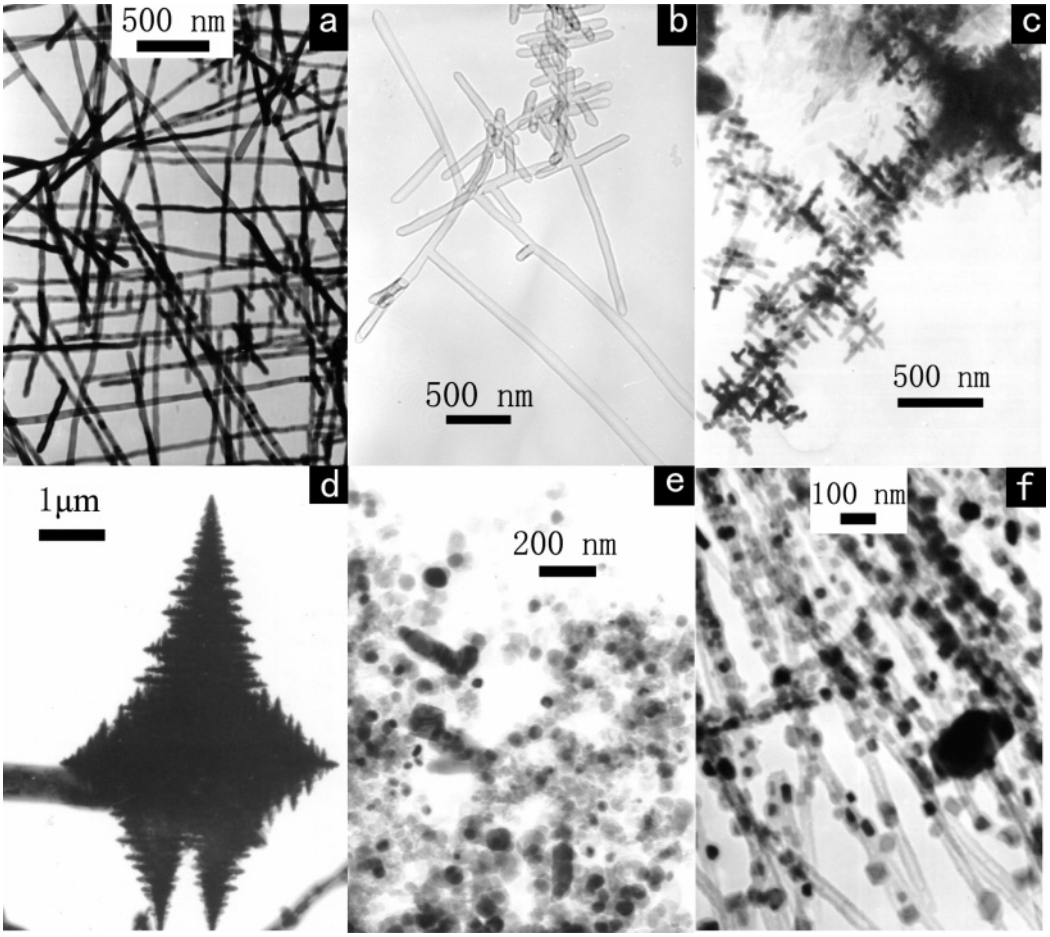

Figure 4. Typical TEM images of samples (a) CM450-1, (b) CT450-1, (c) CM450-2, (d) CM450-3, (e) CM450-4, and (f) CM450-W.

magnetite nanorods can be removed by heating in a mixture of hydrochloric acid−acetic acid to 120 °C, and hollow branched carbon nanotubes (Figure 4b) are obtained, marked as sample CT450-1.

By changing the ratio of the raw material, another typical Fe_3O_4 structure was harvested in samples CM450-5 and CM450-6, the chemical composition of which is confirmed by the XRD pattern, shown in Figure 1b. Figure 3 shows the feature of the microspheres. Formed by interlaced thin Fe_3O_4 nanosheets, the diameter of the spheres is several tens of micrometers. It is interesting that the nanosheets tend to assemble as spheres rather than separated from each other, which may be because of the magnetic properties of Fe_3O_4. It must be mentioned that the samples are not pure. Several branched nanorods can be found on the surface of the spheres, showing that the samples are a mixture of assembled nanosheets and branched nanorods.

The crystallography of the nanostructures is studied with HRTEM. Figure 5 shows the HRTEM image of a part of a branched nanorod. The branch of the coaxial nanowire is vertical to the trunk, connected together with a double-wedge junction. The periodic lattice of different branches and the junction show that the branched Fe_3O_4 core is a single crystal, with each branch having a growth orientation of ⟨100⟩. The trunks and branch have a similar diameter of 30−40 nm, different from normal fractals, dendritics, or other hierarchical structures. A thin amorphous carbon shell (∼6 nm) covers the branched Fe_3O_4 nanorod, which may keep the material stable in air. Correspondingly, the HRTEM image of the nanosheets shows a typical 6-fold lattice. The identity distance shown in Figure 5b is 0.34 nm, corresponding to the (211) facet of magnetite, implicating that the lattice belongs to the (111) facet of magnetite.

We have not obtained a pure sample of either the branched nanorods or assembled nanosheets yet but only a mixture of them. Though lacking the control of the new nanostructures, we found that, by controlling the amount of ferrocene in the raw materials, the ratio of the nanorods and nanosheets can be adjusted. With a certain amount of carbon dioxide, a greater amount of ferrocene (e.g., sample CM450-6) would lead to more nanosheets in the product, while less ferrocene (e.g., sample CM450-1) leads to the harvest of branched nanorods.

On the other hand, a change of the amount of carbon dioxide shows a different influence on the reaction system. Carbon dioxide serves as both a supercritical fluid system and a reactant, so it should be largely excessive in the reaction. A greater amount of carbon dioxide would not affect the reaction distinctly; in contrast, when the density of carbon dioxide is too low to serve as a supercritical solvent, different results may be observed.

Actually, these are the phenomena observed in control experiments. When we reduce the amount of carbon dioxide by half, the length of the Fe_3O_4 nanorods is largely reduced, and the patterns are more similar with fractals, shown in Figure 4c. Further reduction by half leads to the appearance of micrometer-scaled dendrites, shown in Figure 4d. Extremely, by pyrolysis of ferrocene at 450 °C without carbon dioxide, Fe/Fe_3C nanoparticles encapsulated in carbon were obtained in sample CM450-4, shown in Figure 4e. In contrast, by doubling the amount of carbon dioxide, similar branched nanorods are harvested in the production (CM450-7).

Except the sheets and rods, there is little other structure in the product. The main impurity is a kind of discontinuous core−shell nanowire, with Fe_3O_4 nanoparticles discontinuously en-

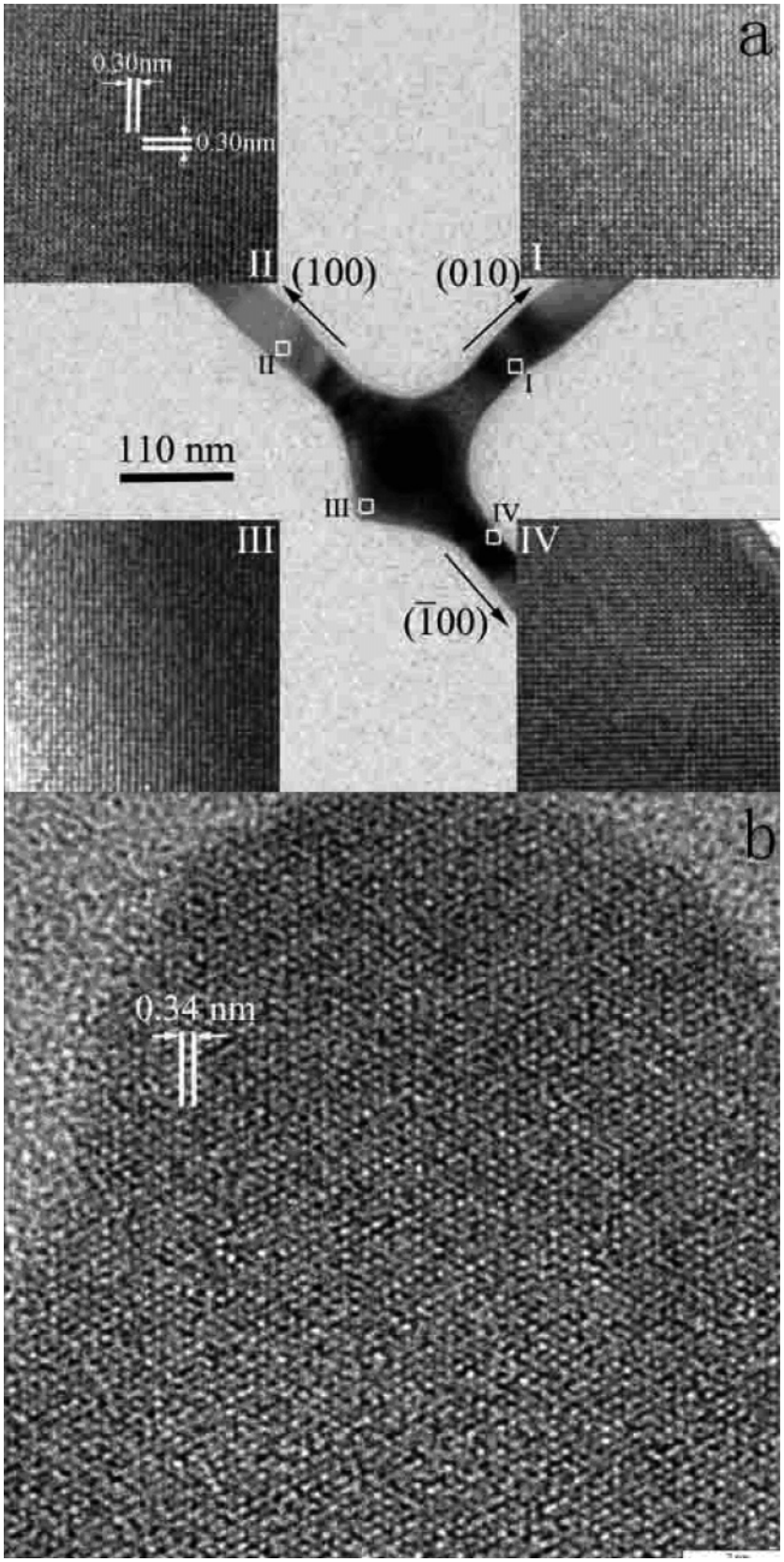

Figure 5. HRTEM images of (a) the branched nanowires and (b) the nanosheets.

capsulated in carbon nanotubes. This was caused by a trace component of H_2O, introduced into the reaction system when CO_2 was changed to dry ice. The hydroxyl in H_2O may adsorb on the Fe atoms in the surface of Fe_3O_4 and stop its growth, making the Fe_3O_4 discontinuous in carbon nanotubes. Experimentally, by adding 0.50 g of H_2O to the reaction system, this discontinuous structure was harvested in sample CM450-8, shown in Figure 4f.

Because ferrocene is very soluble in $ScCO_2$,[17] it is hypothesized that ferrocene is evenly dispersed by $ScCO_2$ under the reaction conditions. It is well-known that Fe^{2+} could be oxidized to Fe^{3+} by CO_2,[18] and Fe_3O_4 is more stable than Fe_2O_3 at the

SCHEME 1: Possible Growth Mechanisms of the Branched Nanorods

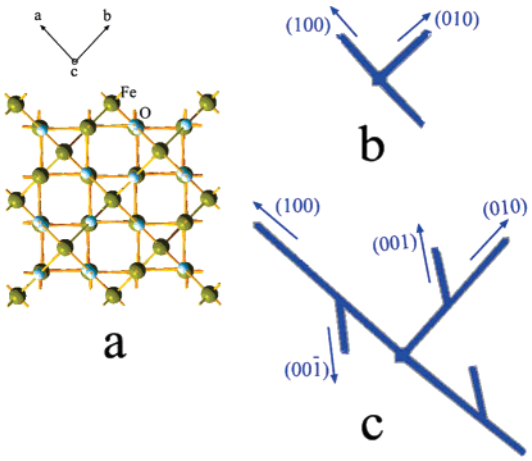

reaction temperature. On the basis of these facts, it is inferred that, in this experiment, the CO_2 molecules react with ferrocene, substituting the cyclopentadienyl group and oxidizing Fe^{2+}. A complex reaction happens among the CO_2 ligand, the central Fe^{2+} cations, and the cyclopentadienyl anions, producing Fe_3O_4, amorphous carbon, and hydrocarbon:

$$FeCp_2 + CO_2 \xrightarrow{450\ ^\circ C} Fe_3O_4 + a\text{-}C + C_nH_m$$

CO_2 is very excessive in the reaction. The concentrated iron oxide was then partially encapsulated by amorphous carbon, forming composite nanoparticles, and then grew longer along a certain crystallographic direction to form nanorods. The diameter of the nanorods is determined by the size of the initial nanoparticles.

It is interesting that there is no branch in the Fe_3O_4/a-C nanorods produced by pyrolyzing ferrocene in $ScCO_2$ at 400 °C,[8] while at 450 °C the branches are well developed. The growth orientations of the two kinds of nanorods are different: the nonbranched nanorods grow along the ⟨110⟩ direction, while the branched one grows along ⟨100⟩. Obviously, the enhancement of the reaction temperature changed the growth rate of different facets of magnetite crystallites. In FC magnetite crystal (Scheme 1a), there are six equivalent ⟨100⟩ directions. For reasons of spatial confinement, one or several of the directions initiates fast growth, and formation of a rod is possible if the growth along these directions is much faster than along the others (Scheme 1b), which approaches nanorods. A dendritic growth[19] may happen during the growth of nanorods, causing subsequent growth along the other crystallographically equivalent directions and leading to the formation of main and possibly symmetric branches on each side. As growth continues, each side branch can initiate growth along other equivalent directions to form subbranches. In the mean time, hydrocarbon fragments carbonize on the surface of Fe_3O_4 and form a carbon shell (Scheme 1c). With further growth, the branched Fe_3O_4 nanorods are covered with the carbon shell and finally encapsulated. As a result, multibranched core−shell nanostructures form.

M−H hysteresis loops (Figure 6) of samples CM450-1, CM450-2, CM450-5, and CM450-7 measured at room temperature show that the powder samples exhibit ferromagnetic characteristics, with corresponding saturation magnetizations $\mathbf{M}_{s1} = 22.0$ emu/g, $\mathbf{M}_{s2} = 49.0$ emu/g, $\mathbf{M}_{s5} = 26.0$ emu/g, and $\mathbf{M}_{s7} = 20.5$ emu/g, respectively. $\mathbf{M}_{s1}$, $\mathbf{M}_{s5}$, and $\mathbf{M}_{s7}$ are smaller than the saturation magnetization of the nonbranched Fe_3O_4/a-C nanorods, which is 27.5 emu/g.[8] Moreover, these $\mathbf{M}_s$ values

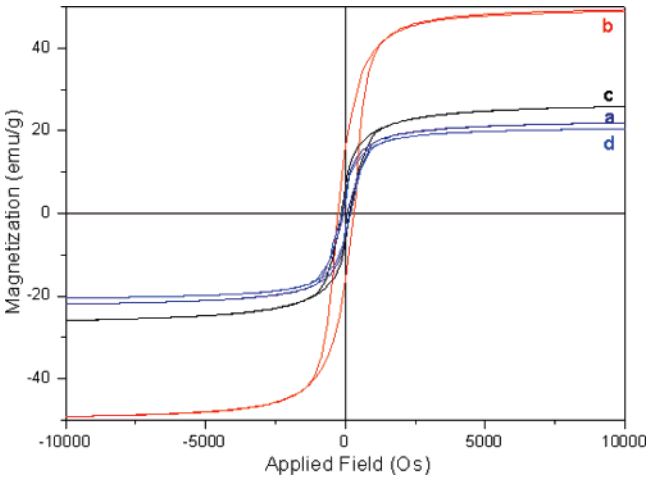

Figure 6. M−H hysteresis loops of samples (a) CM450-1, (b) CM450-2, (c) CM450-5, and (d) CM450-7.

are much lower than the 92 emu/g of bulk magnetite.[20] The reason could be the considerable mass of carbon in the sample and anisotropy of magnetite nanorods.[7a,8] Magnetite nanorods show superparamagnetism when their diameter is near or below the critical size (54 nm) of single domains. The high shape anisotropy of the nanorods prevents them from magnetizing in directions other than along easy magnetic axes; the effect is even stronger in the branched nanorods. With nanorods randomly oriented, the projection of the magnetization vectors along the field direction will be lower than that of nanoparticles without the large shape anisotropy effect. Specially, $\mathbf{M}_{s2}$ is higher than saturation magnetizations of the nonbranched and branched nanorods, which is because there is little shape anisotropic effect in the micrometer-sized particles in sample CM450-2.

Anyway, it is interesting to note that the structures of the dendritics and the branched and core−shell nanorods are converging to a very similar point. Some control of the branched morphology suggests great potential for even larger structures and their utilization in nanoscale devices and systems. For example, similar structures might serve as attractive additives for structural composites or for nanocrystal-based solar cells.[16a]

We also recognize that enhanced knowledge of fundamental factors controlling growth has been crucial to the advances in structural complexity. Potential holds for better control in morphology, purity, and even doping, and much greater complexity may make some exciting applications possible from the bottom-up approach to nanotechnology. Since the starting materials are facile and cheap, and the process is simple, it is envisioned that this approach will be of interest to various fields. The carbon shell can protect magnetite from being oxidized or eroded and strengthen the fragile nanorods, whose magnetic properties may lead to application as probes of magnetic force microscopy.

Conclusions

In this supercritical-fluid-based approach, branched and multilevel branched Fe_3O_4/a-C core−shell nanostructures were produced by pyrolysis of ferrocene in $ScCO_2$ at about 450 °C without a catalyst or surfactant. Fe_3O_4 nanosheets were also found in the product, the amount of which can be controlled by adjusting the ratio of the raw material. This kind of structure is expected to prevent Fe_3O_4 nanorods from being oxidized in external atmospheres and keeps their magnetic performance unchanged. The growth of the morphology suggests great

potential for the synthesis of more complex structures and their utilization in nanoscale devices and systems. A detailed study of the growth mechanism and application is in progress.

Acknowledgment. This work was supported by the Natural Science Foundation of China.

References and Notes

(1) (a) Fert, A.; Piraux, L. *J. Magn. Magn. Mater.* **1999**, *200*, 338. (b) Rodrigues, V.; Bettini, J.; Silva, P. C.; Ugarte, D. *Phys. Rev. Lett.* **2003**, *91*, 096801.

(2) (a) McGary, P. D.; Tan, L. W.; Zou, J.; Stadier, B. J. H.; Downey, P. R.; Flatau, A .B. *J. Appl. Phys.* **2006**, *99*, 08B310. (b) Zhang, D. H.; Liu, Z. Q.; Han, S.; Li, C.; Lei, B.; Stewart, M. P.; Tour, J. M.; Zhou, C. W. *Nano Lett.* **2004**, *4*, 2151.

(3) (a) Sellmyer, D. J.; Zheng, M.; Skomski, R. *J. Phys.: Condens. Matter* **2001**, *13*, R433.(b) Strijkers, G. J.; Dalderop, J. H. J.; Broeksteeg, M. A. A.; Swagten, H. J. M.; de Jonge, W. J. M. *J. Appl. Phys.* **1999**, *86*, 5141.

(4) (a) Cornell, R. M.; Schwertmann, U. *The Iron Oxides*; VCH: New York, 1996. (b) Cheng, F. Y.; Su, C. H.; Yang, Y. S.; Yeh, C. S.; Tsai, C. Y.; Wu, C. L.; Wu, M. T.; Shieh, D. B. *Biomaterials* **2005**, *26*, 729. (c) Soeya, S.; Hayakawa, J.; Takahashi, H.; Ito, K.; Yamamoto, C.; Kida, A.; Asano, H.; Matsui, M. *Appl. Phys. Lett.* **2002**, *80*, 823.

(5) (a) Terrier, C.; Abid, M.; Arm, C.; Serrano-Guisan, S.; Gravier, L.; Ansermet, J.-Ph. *J. Appl. Phys.* **2005**, *98*, 086102. (b) Zhang, L. Y.; Xue, D. S.; Xu, X. F.; Gui, A. B.; Gao, C. X. *J. Phys.: Condens. Matter* **2004**, *16*, 4541.

(6) Yang, J. B.; Xu, H.; You, S. X.; Zhou, X. D.; Wang, C. S.; Yelon, W. B.; James, W. J. *J. Appl. Phys.* **2006**, *99*, 08Q507.

(7) (a) Wang, J.; Chen, Q. W.; Zeng, C.; Hou, B. Y. *Adv. Mater.* **2004**, *16*, 137. (b) Lian, S. Y.; Wang, E. B.; Gao, L.; Kang, Z. H.; Wu, D.; Lan, Y.; Xu, L. *Solid State Commun.* **2004**, *132*, 375.

(8) Cao, F. Y.; Chen, C. L.; Wang, Q.; Chen, Q. W. *Carbon* **2007**, *45*, 727.

(9) Bjork, M. T.; Ohlsson, B. J.; Sass, T.; Persson, A. I.; Thelander, C.; Magnusson, M. H.; Deppert, K.; Wallenberg, L. R.; Samuelson, L. *Nano Lett.* **2002**, *2*, 87.

(10) (a) Lauhon, L. J.; Gudikson, M. S.; Wang, D.; Lieber, C. M. *Nature* **2002**, *420*, 57. (b) Goldberger, J.; He, R.; Zhang, Y.; Lee, S.; Yan, H.; Choi, H. -J.; Yang, P. *Nature* **2003**, *422*, 599.

(11) Cao, M. H.; Liu, T. F.; Gao, S.; Sun, G. B.; Wu, X. L.; Hu, C. W.; Wang, Z. L. *Angew. Chem., Int. Ed.* **2005**, *44*, 4197.

(12) Wang, D. L.; Qian, F.; Yang, C.; Zhong, Z. H.; Lieber, C. L. *Nano Lett.* **2004**, *4*, 871.

(13) Wang, D. L.; Lieber, C. M. *Nat. Mater.* **2003**, *2*, 355.

(14) Kendall, J. L.; Canelas, D. A.; Young, J. L.; DeSimone, J. M. *Chem. Rev.* **1999**, *99*, 543.

(15) (a) Lou, Z. S.; Chen, Q. W.; Zhang, Y. F.; Wang, W.; Qian, Y. T. *J. Am. Chem. Soc.* **2003**, *125*, 9302. (b) Lou, Z. S.; Chen, C. L.; Chen, Q. W.; Gao, J. *Carbon* **2005**, *43*, 1104. (c) Lou, Z. S.; Chen, C. L.; Huang, H. Y.; Zhao, D. J. *Diamond Relat. Mater.* **2006**, *15*, 1540. (d) Wang, Q.; Cao, F. Y.; Chen, Q. W. *Green Chem.* **2005**, *7*, 733.

(16) (a) Huyuh, W. U.; Dittmer, J. J.; Alivisatos, A. P. *Science* **2002**, *295*, 2425. (b) Wen, X. G.; Xie, Y.-T.; Mak, M. W. C.; Cheung, K. Y.; Li, X.-Y.; Renneberg, R.; Yang, S. H. *Langmuir* **2006**, *22*, 4836. (c) Dick, K. A.; Deppert, K.; Karlsoon, L. S.; Seifert, W.; Wallenberg. L. R.; Samuelson, L. *Nano Lett.* **2006**, *6*, 2842.

(17) Cowey, C. M.; Bartle, K. D.; Burford, M. D.; Clifford, A. A.; Zhu, S. *J. Chem. Eng. Data* **1995**, *40*, 1217.

(18) Chen, Q. W.; Bahnemann, D. W. *J. Am. Chem. Soc.* **2000**, *122*, 970.

(19) Ould-Ely, T.; Prieto-Centurion, D.; Kumar, A.; Guo, W.; Knowles, W. V.; Asokan, S.; et al. *Chem. Mater.* **2006**, *18*, 1821.

(20) Wang, J.; Peng, Z. M.; Huang, Y. J.; Chen, Q. W. *J. Cryst. Growth* **2004**, *263*, 616.